

## RESEARCH ARTICLE

# The water channel aquaporin-1a1 facilitates movement of CO<sub>2</sub> and ammonia in zebrafish (*Danio rerio*) larvae

Krystle Talbot, Raymond W. M. Kwong, Kathleen M. Gilmour\* and Steve F. Perry

## ABSTRACT

The present study tested the hypothesis that zebrafish (*Danio rerio*) aquaporin-1a1 (AQP1a1) serves as a multi-functional channel for the transfer of the small gaseous molecules, CO<sub>2</sub> and ammonia, as well as water, across biological membranes. Zebrafish embryos were microinjected with a translation-blocking morpholino oligonucleotide targeted to AQP1a1. Knockdown of AQP1a1 significantly reduced rates of CO<sub>2</sub> and ammonia excretion, as well as water fluxes, in larvae at 4 days post fertilization (dpf). Because AQP1a1 is expressed both in ionocytes present on the body surface and in red blood cells, the haemolytic agent phenylhydrazine was used to distinguish between the contributions of AQP1a1 to gas transfer in these two locations. Phenylhydrazine treatment had no effect on AQP1a1-linked excretion of CO<sub>2</sub> or ammonia, providing evidence that AQP1a1 localized to the yolk sac epithelium, rather than red blood cell AQP1a1, is the major site of CO<sub>2</sub> and ammonia movements. The possibility that AQP1a1 and the rhesus glycoprotein Rhcg1, which also serves as a dual CO<sub>2</sub> and ammonia channel, act in concert to facilitate CO<sub>2</sub> and ammonia excretion was explored. Although knockdown of each protein did not affect the abundance of mRNA and protein of the other protein under control conditions, impairment of ammonia excretion by chronic exposure to high external ammonia triggered a significant increase in the abundance of AQP1a1 mRNA and protein in 4 dpf larvae experiencing Rhcg1 knockdown. Collectively, these results suggest that AQP1a1 in zebrafish larvae facilitates the movement of CO<sub>2</sub> and ammonia, as well as water, in a physiologically relevant fashion.

**KEY WORDS:** CO<sub>2</sub> excretion, Ammonia excretion, Aquaporin, Rh glycoprotein, High external ammonia

## INTRODUCTION

In the past decade, models of the processes underlying the transfer of small gaseous molecules across biological membranes have been significantly revised to include the movement of gases through membrane channel proteins (Wright and Wood, 2009; Boron, 2010; Endeward et al., 2014). Members of two multigene families, the aquaporins and the rhesus (Rh) glycoproteins, appear to be capable of facilitating the movements of both CO<sub>2</sub> and ammonia and in fact exhibit characteristic selectivities for CO<sub>2</sub> versus NH<sub>3</sub> (Musa-Aziz et al., 2009; Geyer et al., 2013a,b). These conclusions are not, however, without controversy, particularly with respect to the movement of CO<sub>2</sub> (for discussion, see Missner and Pohl, 2009; Boron et al., 2011; de Groot and Hub, 2011; Endeward et al., 2014). Although the weight of experimental evidence suggests that CO<sub>2</sub> can

indeed move through aquaporins and Rh proteins, the question of whether these channels are physiologically important to CO<sub>2</sub> movement remains open (Endeward et al., 2014). Of central importance to this question is the intrinsic permeability of a cell membrane to CO<sub>2</sub>; there would be little to be gained from the presence of gas channels if the non-gas-channel portion of the membrane is highly permeable to CO<sub>2</sub>. However, while the CO<sub>2</sub> permeability of phospholipid bilayers lacking cholesterol is relatively high, the presence of typical amounts of cholesterol (30–50 mol% of total lipid) is sufficient to lower CO<sub>2</sub> permeability to the range where gas channels could be functionally relevant (Itel et al., 2012; Tsiavaliaris et al., 2015). For example, the CO<sub>2</sub> permeability of Madin–Darby canine kidney (MDCK) cells, which lack aquaporin-1 (AQP1) and contain 37 mol% cholesterol in membrane lipids, increased by 50% when the cells were stably transfected with a construct containing human AQP1 (Itel et al., 2012).

*In vivo* work assessing the physiological relevance of gas channels in CO<sub>2</sub> metabolism is sparse and has yielded mixed results. Use of AQP1-knockout mice as a model to study CO<sub>2</sub> permeability in red blood cells (RBCs), lung and kidney could not confirm a role for AQP1 (Yang et al., 2000; Fang et al., 2002). However, it has been suggested that issues with the experimental conditions might have made it difficult to detect a contribution of AQP1 to CO<sub>2</sub> permeability in these studies (Endeward et al., 2014). Preliminary data cited by Boron (2010) suggest that exercise capacity is reduced in AQP1-knockout mice (Xu et al., 2010), although this effect has yet to be linked explicitly to the absence of AQP1 from RBCs, and that CO<sub>2</sub> absorption by the proximal tubule of the kidney is 60% lower in AQP1-knockout than wild-type mice (Zhou et al., 2006). In plants, the physiological importance of AQP1 is evident; CO<sub>2</sub> is the substrate during photosynthetic carbon fixation and overexpression of tobacco plant AQP1 increased the net photosynthesis rate of the plants ~1.5-fold (Uehlein et al., 2003). In zebrafish larvae, translational knockdown of Rh proteins provided *in vivo* evidence implicating Rh proteins in movement of CO<sub>2</sub> as well as ammonia (Perry et al., 2010). Elimination of CO<sub>2</sub> occurs across the body surface in larval fish; the gills only become significant for gas transfer in developing zebrafish around 14 days post-fertilization (dpf) (Rombough, 2002). Using microrespirometry techniques, Perry et al. (2010) measured rates of CO<sub>2</sub> excretion ( $\dot{M}_{CO_2}$ ) for 4 dpf larval zebrafish, expressing  $\dot{M}_{CO_2}$  relative to rates of O<sub>2</sub> uptake ( $\dot{M}_{O_2}$ ) to control for changes in metabolism. This calculation yields the respiratory exchange ratio (RER= $\dot{M}_{CO_2}/\dot{M}_{O_2}$ ). Knockdown of the epithelial Rh proteins Rhcg1 or Rhbg, treatments that are known to reduce ammonia excretion (Braun et al., 2009a), significantly decreased RER, implying relative inhibition of CO<sub>2</sub> excretion (Perry et al., 2010). The reduction of RER in larvae experiencing knockdown of both Rhcg1 and Rhbg was substantial; RER was ~50% of that for sham-injected larvae (Perry et al., 2010). Thus, it appears that members of the Rh protein family contribute in a physiologically significant fashion to both CO<sub>2</sub> and ammonia

Department of Biology, University of Ottawa, Ottawa, Ontario K1N 6N5, Canada.

\*Author for correspondence (kgilmour@uottawa.ca)

Received 6 August 2015; Accepted 19 October 2015

**Symbols and abbreviations**

AQP1	aquaporin-1
AQP1a1-MO	AQP1a1 morphant
ar/R	aromatic/arginine
HEA	high external ammonia
HR cell	V-type H <sup>+</sup> -ATPase-rich cell
HRP	horseradish peroxidase
$J_{\text{amm}}$	ammonia excretion
$\dot{M}_{\text{CO}_2}$	rate of CO <sub>2</sub> excretion
MDCK	Madin–Darby canine kidney
$\dot{M}_{\text{O}_2}$	rate of O <sub>2</sub> consumption
MS-222	tricaine methanesulphonate
NaR cell	Na <sup>+</sup> ,K <sup>+</sup> -ATPase-rich cell
NPA	asparagine-proline-alanine
PHZ	phenylhydrazine
$P_{\text{O}_2}$	partial pressure of O <sub>2</sub>
PVDF	polyvinylidene difluoride
RBC	red blood cell
RER	respiratory exchange ratio ( $\dot{M}_{\text{CO}_2}/\dot{M}_{\text{O}_2}$ )
Rh	Rhesus
Rhcg1-MO	Rhcg1 morphant

excretion in larval zebrafish. The goal of the present study was to evaluate whether AQP1 also contributes to both CO<sub>2</sub> and ammonia excretion *in vivo* in larval zebrafish.

To date, 18 gene sequences that are related to four different AQP families have been identified in zebrafish, including two genes encoding AQP1 paralogs, *aqp1a1* and *aqp1a2* (Tingaud-Sequeira et al., 2010). Aquaporin-1a2 is expressed only in the brain, testis and ovary (Tingaud-Sequeira et al., 2010), and in marine teleosts is required for full hydration of oocytes undergoing meiotic maturation (Zapater et al., 2011). Aquaporin-1a2 is unlikely to contribute significantly to gas homeostasis in freshwater zebrafish larvae. By contrast, *in situ* hybridization studies demonstrated *aqp1a1* expression in the vasculature, in RBCs, and in the skin covering the yolk sac of larval zebrafish, locations in which it could potentially contribute to gas transfer (Chen et al., 2010). The yolk sac epithelium contains at least two types of ion-transporting cells, or ionocytes, that express AQP1a1 as early as 4 dpf: the V-type H<sup>+</sup>-ATPase-rich (HR) cells and the Na<sup>+</sup>,K<sup>+</sup>-ATPase-rich (NaR) cells (Kwong et al., 2013). Moreover, expression of zebrafish *aqp1a1* in *Xenopus* oocytes established that AQP1a1 was permeable to both CO<sub>2</sub> and ammonia (Chen et al., 2010).

Given the expression of AQP1a1 on the yolk sac epithelium, the cutaneous excretion of CO<sub>2</sub> and ammonia during early development, and the evidence supporting AQP1a1 as a dual conduit for CO<sub>2</sub> and ammonia, the present study tested the hypothesis that AQP1a1 contributes to CO<sub>2</sub> and ammonia excretion in larval zebrafish. Several predictions arise from this hypothesis. Most importantly, functional knockdown of AQP1a1 would be predicted to reduce  $\dot{M}_{\text{CO}_2}$  and hence RER, as well as ammonia excretion ( $J_{\text{amm}}$ ). Exposure to high external ammonia (HEA) concentrations, which favour ammonia loading into tissues and inhibit  $J_{\text{amm}}$  (Braun et al., 2009b), is predicted to increase AQP1a1 abundance as a compensatory mechanism to excrete the excess ammonia. In addition, if AQP1a1 and Rhcg1 act in concert to facilitate CO<sub>2</sub> and ammonia movements across the larval body surface, then knockdown of AQP1a1 would be predicted to trigger a compensatory increase in Rhcg1 mRNA and protein expression. Similarly, a compensatory increase in AQP1a1 mRNA and protein abundance would be predicted to occur in larvae experiencing knockdown of Rhcg1.

**MATERIALS AND METHODS****Experimental animals**

Adult zebrafish [*Danio rerio* (Hamilton 1822)] were purchased from Big Al's Aquarium Services (Ottawa, ON, Canada) and housed in the University of Ottawa's Aquatic Care Facility. The fish were held in tanks supplied with aerated, flowing, city of Ottawa dechloraminated tap water at 28°C, subjected to a constant 14 h light:10 h dark photoperiod, and fed daily with No. 1 Crumble (Zeigler, Gardners, PA, USA). Embryos were obtained using standard breeding procedures (Westerfield, 2000), and were raised in 50 ml Petri dishes containing E3 medium (5 mmol l<sup>-1</sup> NaCl, 0.17 mmol l<sup>-1</sup> KCl, 10 mmol l<sup>-1</sup> HEPES, 0.33 mmol l<sup>-1</sup> CaCl<sub>2</sub>, 0.33 mmol l<sup>-1</sup> MgSO<sub>4</sub>, 0.0001% methylene blue) and held in incubators kept at 28°C. Dead embryos were removed and medium was refreshed daily. All analyses were performed at 4 days post fertilization (dpf) and therefore larvae were not fed for the duration of the experiments. All procedures were conducted in compliance with University of Ottawa institutional guidelines, were approved by the Animal Care Committee (protocol BL-226), and were in accordance with the guidelines of the Canadian Council on Animal Care for the use of animals in research and teaching.

**Experimental series**

Four experimental series were carried out. The goal of the first series was to determine whether functional knockdown of AQP1a1 affected CO<sub>2</sub> and/or ammonia excretion. In the second experimental series, phenylhydrazine treatment was used to eliminate RBCs to distinguish between contributions of AQP1a1 on RBCs and AQP1a1 on the yolk sac epithelium. The third experimental series explored the possibility of interactions between AQP1a1 and Rhcg1. Finally, the contribution of AQP1a1 to CO<sub>2</sub> and ammonia excretion was assessed under conditions designed to impair ammonia excretion, exposure to HEA with and without functional knockdown of Rhcg1.

**Series I: effects of AQP1a1 knockdown on excretion of CO<sub>2</sub> and ammonia**

The methods used to achieve and confirm functional knockdown of AQP1a1 were similar to those used by Kwong et al. (2013). In brief, an antisense morpholino oligonucleotide (5'-AAG CCT TGC TCT TCA GCT CGT TCA T-3'; Genetools, OR, USA) designed to be complementary to the translational start site of zebrafish AQP1a1 (GenBank NM 207059.1) was prepared to a final concentration of 4 ng nl<sup>-1</sup> in 1× Danieau buffer [58 mmol l<sup>-1</sup> NaCl, 0.7 mmol l<sup>-1</sup> KCl, 0.4 mmol l<sup>-1</sup> MgSO<sub>4</sub>, 0.6 mmol l<sup>-1</sup> Ca(NO<sub>3</sub>)<sub>2</sub>, 5.0 mmol l<sup>-1</sup> HEPES, adjusted to pH 7.6] containing 0.05% (v/v) Phenol Red (as a visible indicator of successful injection). The morpholino (4 ng per embryo) was microinjected (model IM 300; Narishige, Long Island, NY, USA) into embryos at the one- to two-cell stage. To control for possible effects of microinjection, 'sham' embryos were injected with a standard (control) morpholino from GeneTools (5'-CCT CTT ACC TCA GTT ACA ATT TAT A-3') at the same concentration; there is no known target sequence in zebrafish for this morpholino. Neither obvious morphological deformities nor substantial mortality was observed following AQP1a1 knockdown.

To confirm successful knockdown of AQP1a1, AQP1a1 protein levels were assessed by western blotting and immunohistochemistry, and *in vivo* water influx rates were assessed isotopically. For western blot analysis ( $N=4$ ), pools of 20 larvae ( $N=1$ ) were homogenized in RIPA buffer (150 mmol l<sup>-1</sup> NaCl, 1% Triton X-100, 0.5% sodium deoxycholate, 0.1% SDS, 50 mmol l<sup>-1</sup> Tris-HCl, 1 mmol l<sup>-1</sup> EDTA, 1 mmol l<sup>-1</sup> phenylmethanesulphonyl fluoride) containing a protease inhibitor cocktail (Roche, Laval, QC, Canada). Extracted protein was mixed 1:1 with Laemmli sample buffer (Sigma-Aldrich, Oakville, ON, Canada), heated for 10 min at 65°C, size-fractionated on a 12% SDS-PAGE gel and then transferred (Trans-Blot SD transfer system; Bio-Rad, Mississauga, ON, Canada) to a polyvinylidene difluoride (PVDF) membrane. Membranes were blocked for 1 h at room temperature with 5% skimmed milk powder in TBST (20 mmol l<sup>-1</sup> Tris-HCl, 300 mmol l<sup>-1</sup> NaCl, 0.05% Tween 20, pH 7.5) and then probed overnight at 4°C using a 1:1000 dilution in 2% skimmed milk in TBST of an antibody raised against a 15 amino acid residue in eel (*Anguilla anguilla*) AQP1a1 (VNGPDDVPAVEMSSK; 87% identity with zebrafish AQP1a1 over the

corresponding region of the C-terminal; the antibody was a kind gift from Dr G. Cramb, University of St. Andrews, Scotland). This antibody detects a single band at ~27 kDa in 4 dpf zebrafish larvae (Kwong et al., 2013). Membranes were washed with TBST (3×5 min) and incubated with a 1:5000 dilution of horseradish-peroxidase (HRP) goat anti-rabbit IgG (Pierce, Rockford, IL, USA) for 2 h at room temperature. After a final wash in TBST (3×15 min), bands were detected using Luminata Western HRP substrates (Millipore, Fisher Scientific, Ottawa, ON, Canada). To control for protein loading, membranes were stripped with Re-Blot Plus solution (Millipore, USA) used according to the manufacturer's instructions and re-probed with a 1:4000 dilution of anti-β-actin (A2066, Sigma-Aldrich). Quantification of band density was performed using ImageJ software (<http://imagej.nih.gov/ij/>) and AQP1a1 protein expression was normalized to that of β-actin.

Measurement of water influx rate was used as a second method of confirming successful knockdown of AQP1a1 ( $N=5-6$ ). Groups of sham and AQP1a1 morphant (AQP1a1-MO) larvae were exposed separately to  $1 \mu\text{Ci ml}^{-1}$  of  $^3\text{H}_2\text{O}$  (American Radiolabeled Chemicals, St Louis, MO, USA) for 4 h. Larvae were then killed by immersion in a solution of tricaine methanesulphonate (MS-222;  $250 \text{ mg l}^{-1}$ ; Argent Chemical Laboratories, Redmond, WA, USA), washed in isotope-free water, and pooled into groups of three as one sample ( $N=1$ ). Water samples ( $50 \mu\text{l}$ ) were also collected at the beginning and end of the flux period to determine the specific activity of  $^3\text{H}_2\text{O}$ . Fish were digested with a tissue solubilizer ( $80 \mu\text{l}$ ; Solvable™; Perkin Elmer, Waltham, MA, USA) and neutralized with glacial acetic acid (~0.4 ml) before addition of scintillation cocktail (5 ml; BioSafe-II; RPI, Mt. Prospect, IL, USA). Radioactivity of the digested fish and water samples was quantified using a liquid scintillation counter (LS-6500; Beckman Coulter, Mississauga, ON, Canada). Influx of  $^3\text{H}_2\text{O}$  was calculated by dividing the radioactivity of the fish by the specific activity of the water, number of fish, and duration of the experiment.

Immunohistochemistry using the eel anti-AQP1a1 antibody was carried out as a qualitative method of confirming knockdown and to examine the localization of AQP1a1 in larvae. Larvae (sham and AQP1a1-MO) were killed as described above and fixed overnight at  $4^\circ\text{C}$  in a solution of 4% paraformaldehyde prepared in phosphate-buffered saline (PBS;  $137 \text{ mmol l}^{-1}$  NaCl,  $2.7 \text{ mmol l}^{-1}$  KCl,  $10 \text{ mmol l}^{-1}$   $\text{Na}_2\text{HPO}_4$ ,  $1.8 \text{ mmol l}^{-1}$   $\text{KH}_2\text{PO}_4$ ). Following fixation, samples were washed with PBST (PBS containing 0.1% Tween-20) and heated for 10 min at  $65^\circ\text{C}$  in  $150 \text{ mmol l}^{-1}$  Tris buffer (pH 9) to improve antigen retrieval. Samples were washed again in PBST, blocked for 1 h at room temperature in PBST containing 10% goat serum (Jackson ImmunoResearch, West Grove, PA, USA) and 0.4% Triton X-100, and incubated overnight at  $4^\circ\text{C}$  with a 1:250 dilution (also in 10% goat serum) of the AQP1a1 antibody. Subsequently, samples were incubated for 2 h at room temperature, in the dark, with a 1:500 dilution of Alexa-488-conjugated goat anti-rabbit IgG (Invitrogen, Burlington, ON, Canada). Samples were examined using an AIR+ A1+ Nikon confocal microscope (Nikon Instruments, Melville, NY, USA).

Closed-system microrespirometry was carried out on groups of 30 larvae ( $N=1$ ) to measure  $\dot{M}_{\text{CO}_2}$ ,  $\dot{M}_{\text{O}_2}$  ( $N=7$ ) and  $J_{\text{amm}}$  ( $N=12-13$ ). Sham or AQP1a1-MO larvae were placed in glass microrespirometry chambers (internal volume of 2 ml; Loligo Systems, Tjele, Denmark). The chambers were paired with a mini-magnetic stirring system (Loligo) utilizing a magnetic stir bar placed within the microrespirometry chamber but separated from the larvae by a steel mesh. The microrespirometry chambers were partially submerged in a water bath containing  $28^\circ\text{C}$  water. A fibre-optic  $\text{O}_2$  electrode (FOXY AL-300; Ocean Optics, Dunedin, FL, USA) was used to monitor the partial pressure of  $\text{O}_2$  ( $P_{\text{O}_2}$ ) within the chamber. Prior to each experimental run, electrodes were calibrated using zero solution ( $2 \text{ g l}^{-1}$  sodium sulphite) and air-equilibrated water. Water samples ( $50 \mu\text{l}$ ) were removed from the microrespirometry chamber using gas-tight Hamilton syringes and total  $\text{CO}_2$  content was measured in triplicate using a custom-built total  $\text{CO}_2$  analyser with a detection limit of  $6.8 \mu\text{mol l}^{-1}$  (0.3 ppm). The  $\text{CO}_2$  analyser was calibrated using a  $1 \text{ mmol l}^{-1}$  solution of  $\text{NaHCO}_3$ . The design of the total  $\text{CO}_2$  analyser was based upon the Capni-Con Total  $\text{CO}_2$  Analyser from Cameron Instruments; the instrument was designed and built by the electronics shop of the Faculty of Science at the University of Ottawa.

Each experimental run began with the placement of a group of either sham or AQP1a1-MO larvae into the microrespirometry chamber. Initial water samples were removed for total  $\text{CO}_2$  analysis, the chamber was sealed, and  $P_{\text{O}_2}$  was monitored continuously for 30 min, at which time final water samples were removed for analysis of total  $\text{CO}_2$  content. The rate of change of  $P_{\text{O}_2}$  within the chamber was used to calculate  $\dot{M}_{\text{O}_2}$ , taking into account chamber volume, mass of the larvae and the solubility coefficient of  $\text{O}_2$  in fresh water at  $28^\circ\text{C}$  (Boutilier et al., 1984). The difference in total  $\text{CO}_2$  content between initial and final water samples was used to calculate  $\dot{M}_{\text{CO}_2}$ , taking into account chamber volume, duration of the closed-chamber flux period and mass of the larvae. In separate trials, a similar calculation yielded  $J_{\text{amm}}$ , but used ammonia concentrations for water samples collected at the beginning and end of the closed-chamber flux period. Water ammonia concentrations were measured using a microplate version of the colorimetric assay of Verdouw et al. (1978).

### Series II: distinguishing between possible sites of AQP1a1-facilitated gas movement

To address the question of whether RBC or yolk sac epithelium AQP1a1 primarily is involved in  $\text{CO}_2$  and ammonia movements, phenylhydrazine (PHZ) was used to induce haemolytic anaemia (Pelster and Burggren, 1996). Developing sham or AQP1a1-MO zebrafish were exposed to either  $0.4 \text{ mg l}^{-1}$  PHZ or control water from 1 to 4 dpf; Petri dishes of developing zebrafish for these trials were held in a dark  $28^\circ\text{C}$  incubator because PHZ is photosensitive. Closed-system microrespirometry was carried out as described above to measure  $\dot{M}_{\text{O}_2}$ ,  $\dot{M}_{\text{CO}_2}$  ( $N=5$ ), and in separate trials,  $J_{\text{amm}}$  ( $N=5$ ). To confirm the effectiveness of PHZ in inducing anaemia, control and PHZ-treated larvae were killed, fixed overnight at  $4^\circ\text{C}$  in 4% PFA, washed in PBS and then stained for 10 min in the dark in a solution of *o*-dianisidine ( $0.6 \text{ mg ml}^{-1}$ ),  $0.01 \text{ mol l}^{-1}$  sodium acetate (pH 4.5), 0.65%  $\text{H}_2\text{O}_2$  and 40% (v/v) ethanol as described by Detrich et al. (1995). Excess stain was removed in a series of PBS washes ( $3 \times 1 \text{ ml}$ ) and patterns of globin staining were observed in samples using an SMZ1500 microscope (Nikon Instruments).

### Series III: is there a functional relationship between AQP1a1 and Rhcg1?

To study the possibility of interactions between AQP1a1 and Rhcg1, AQP1a1 expression was examined in Rhcg1 morphant (Rhcg1-MO) larvae, and Rhcg1 expression was examined in AQP1a1-MO, at both the mRNA and protein levels. Zebrafish embryos were microinjected with either the AQP1a1 morpholino or with a morpholino oligonucleotide (5'-TTG GTG TTT TTT ACC ATT TTT GAT C-3') designed to inhibit the translation of zebrafish *rhcg1* (also known as *rhcgB*; GenBank AB286865.1) as described and validated by Braun et al. (2009a). In either case, a corresponding 'sham' group of embryos was microinjected with a standard (control) morpholino (GeneTools). Effectiveness of the AQP1a1 morpholino was confirmed as described above. Confirmation of Rhcg1 knockdown was achieved by measuring  $J_{\text{amm}}$  for sham and Rhcg1-MO larvae ( $N=4$ ), using the methods described above.

Protein abundance of Rhcg1 in sham and AQP1a1-MO larvae ( $N=6-7$ ) was measured by western blotting (see above) using a polyclonal rabbit antibody (1:1000 dilution) developed against zebrafish Rhcg1 (see Nakada et al., 2007) and kindly donated by Prof. S. Hirose (Tokyo Institute of Technology, Japan). Similarly, AQP1a1 protein abundance was measured by western blotting (as above) in sham and Rhcg1-MO larvae ( $N=4-5$ ).

To measure mRNA abundance, groups of 20 ( $N=1$ ) sham, AQP1a1-MO or Rhcg1-MO larvae ( $N=6$ ) were collected, killed and immediately flash-frozen in liquid nitrogen before being stored at  $-80^\circ\text{C}$  until analysis. Total RNA was extracted from pooled larvae using TRIzol (Invitrogen), treated with DNase I (Invitrogen) according to the manufacturer's instructions and quantified using a NanoDrop ND2000 UV-Vis spectrophotometer (Thermo Scientific, Ottawa, ON, Canada). To generate cDNA,  $1 \mu\text{g}$  RNA was reverse transcribed using RevertAid M-MuLV reverse transcriptase (Fermentas, Burlington, ON, Canada) and  $0.2 \mu\text{g} \mu\text{l}^{-1}$  of random hexamer primer (ReadyMade Primer; IDT, Coralville, IA, USA) according to the manufacturer's protocol. Semi-quantitative real-time RT-PCR was carried out using a real-time PCR cycler (CFX96; Bio-Rad) with Brilliant III SYBR Green Master Mix (Agilent Technologies, Santa Clara, CA, USA). The

manufacturer's instructions were followed with the exception that the total volume was scaled to 10  $\mu\text{l}$  instead of 25  $\mu\text{l}$ . Gene-specific primers for *rhcg1* (forward, 5'-TTT GGA GGA GAG GCT GAA GA-3'; reverse, 5'-CGA AAC ACA AGG CCA CAC AC-3') were designed using Primer3 software (<http://frodo.wi.mit.edu/primer3/>) and the PCR product was confirmed by direct sequencing. Primers for *aqp1a1* (forward, 5'-GCG ACT GTG GCC AGC GCT AT-3'; reverse, 5'-CGT CCC GCC GCC TTT TGT CT-3') were from Kwong et al. (2013) and the ribosomal 18S subunit (GenBank FJ915075.1) was used as a reference gene with primers (forward, 5'-GGC GGC GTT ATT CCC ATG ACC-3'; reverse, 5'-GGT GGT GCC CTT CCG TCA ATT C-3') from Kumai and Perry (2011). The conditions for all experiments were 95°C for 3 min, 40 cycles of 95°C for 20 s and 60°C for 20 s, with 5 min for a final extension at 72°C. The cDNA samples were diluted 1:1000 for 18S or 1:5 for *aqp1a1* and *rhcg1*. Each sample was assayed in duplicate, and no-reverse-transcriptase controls (samples from which reverse transcriptase was omitted during cDNA synthesis) and no-template controls (samples from which RNA was omitted during cDNA synthesis) were generated and run in parallel with the samples. Standard curves were generated for each gene using pooled sham and morphant samples, and reaction compositions were adjusted to optimize the efficiency of the reaction. Following the completion of 40 cycles, SYBR green dissociation curves were used to confirm the presence of single amplicons for each primer pair. All data were normalized against expression of the housekeeping gene (18S), and expressed relative to the corresponding sham group using a modification of the  $\Delta\Delta C_t$  method (Pfaffl, 2001).

#### Series IV: challenging AQP1a1 with exposure to high external ammonia (HEA)

Wild-type embryos were raised from 1 to 4 dpf either in control water or in water containing HEA (500  $\mu\text{mol l}^{-1}$   $\text{NH}_4\text{Cl}$ ), a treatment that elevates whole body ammonia levels and impairs ammonia excretion (Braun et al., 2009b). Using samples of 20 larvae ( $N=1$ ), AQP1a1 mRNA ( $N=7$ ) and protein ( $N=8$ ) abundances were quantified by real-time RT-PCR (note that expression of the reference gene 18S was not affected by HEA) and western blotting, respectively, as described above. If Rhcg1 and AQP1a1 act in concert to facilitate  $\text{CO}_2$  and ammonia excretion, then knockdown of Rhcg1

should increase the burden of gas transfer through AQP1a1, resulting in greater fluctuations in AQP1a1 mRNA and protein expression in response to HEA. To test this prediction, HEA experiments were repeated on sham and/or Rhcg1-MO larvae ( $N=6$  for sham and  $N=11$ –12 for Rhcg1-MO larvae for mRNA abundance, and  $N=6$  for protein abundance).

#### Statistical analyses

Data are presented as mean values  $\pm$  s.e.m. Effects of gene knockdown or HEA on mRNA or protein abundances were assessed using one-sample Student's *t*-tests. Comparisons of water flux,  $\dot{M}_{\text{O}_2}$ ,  $\dot{M}_{\text{CO}_2}$ , RER and  $J_{\text{amm}}$  between sham and AQP1a1-MO larvae were carried out using Student's *t*-tests. Two-way analysis of variance (ANOVA) was used to test for effects of AQP1a1 knockdown and phenylhydrazine treatment, with *post hoc* testing carried out using the Holm–Šidák method. Statistical analyses were carried out using SigmaPlot v11 (Systat Software, Chicago, IL, USA) with a fiducial limit of significance of 0.05.

## RESULTS

### Series I: effects of AQP1a1 knockdown on excretion of $\text{CO}_2$ and ammonia

The effectiveness of the morpholino knockdown of AQP1a1 protein expression was supported by significantly lower AQP1a1 protein abundance (Fig. 1A;  $P<0.001$ , one-sample Student's *t*-test) and influx of tritiated water (Fig. 1B;  $P=0.004$ , Student's *t*-test) in AQP1a1-MO relative to sham larvae. Qualitatively, immunofluorescence associated with AQP1a1 in the RBCs of the heart, vasculature and gill of sham larvae was markedly reduced in AQP1a1-MO larvae (Fig. 1C). Knockdown of AQP1a1 significantly reduced  $\dot{M}_{\text{CO}_2}$  by approximately 35% in the absence of any significant impact on  $\dot{M}_{\text{O}_2}$  (Fig. 2A;  $P<0.001$  and  $P=0.331$  for  $\dot{M}_{\text{CO}_2}$  and  $\dot{M}_{\text{O}_2}$ , respectively, Student's *t*-tests). The specific impairment of  $\text{CO}_2$  excretion was confirmed by the significantly lower RER of AQP1a1-MO relative to sham larvae (Fig. 2B,  $P=0.047$ , Student's *t*-test). Knockdown of AQP1a1 also significantly reduced  $J_{\text{amm}}$  by approximately 31% (Fig. 3;  $P=0.018$ , Student's *t*-test).

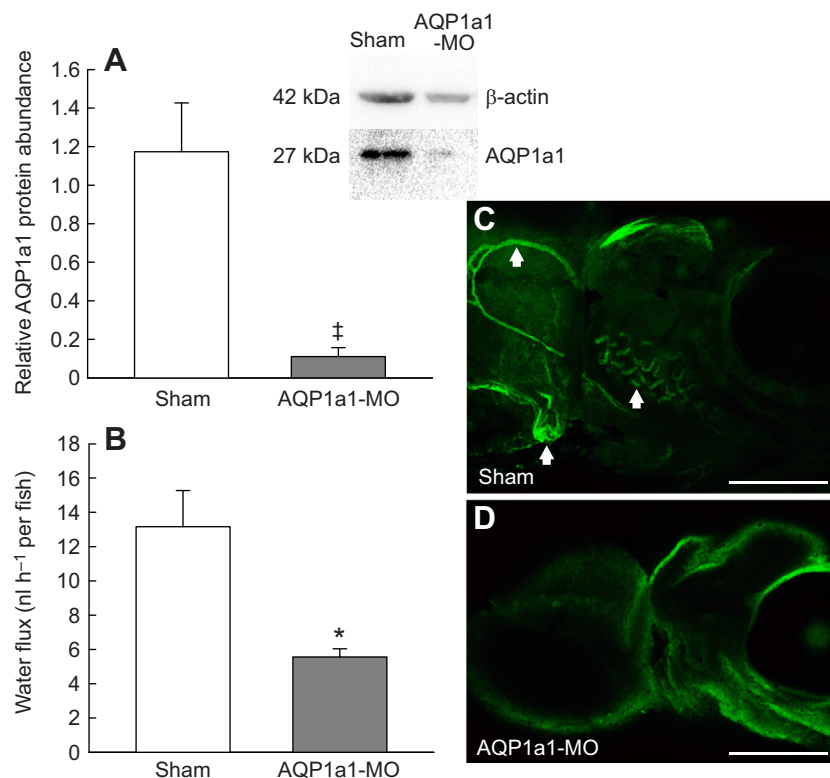


**Fig. 1. Confirmation of AQP1a1 knockdown in 4 dpf larval zebrafish (*Danio rerio*) microinjected with an AQP1a1 morpholino as one- to two-cell embryos (series I).** (A) The protein abundance of AQP1a1 was significantly lower in AQP1a1 morphants (AQP1a1-MO) relative to sham larvae as determined by western blotting ( $^{\dagger}P<0.001$ , one-sample Student's *t*-test). The inset shows bands from a representative western blot illustrating the protein expression of AQP1a1 in lysates of 4 dpf sham and AQP1a1-MO relative to corresponding protein expression of  $\beta$ -actin. (B) Water influx was significantly lower in AQP1a1-MO relative to sham larvae ( $^*P=0.004$ , Student's *t*-test). Values are means  $\pm$  s.e.m. with  $N=4$  for and  $N=5$ –6 for B; symbols indicate statistical significance. (C, D) Fluorescent immunohistochemistry and confocal microscopy revealed the expression of AQP1a1 in areas of blood flow including the heart (lower left of image), gill (middle of image) and pectoral artery (upper left of image); all three areas are indicated with arrows) in sham (C) but not AQP1a1-MO larvae (D). Scale bars: 200  $\mu\text{m}$ .

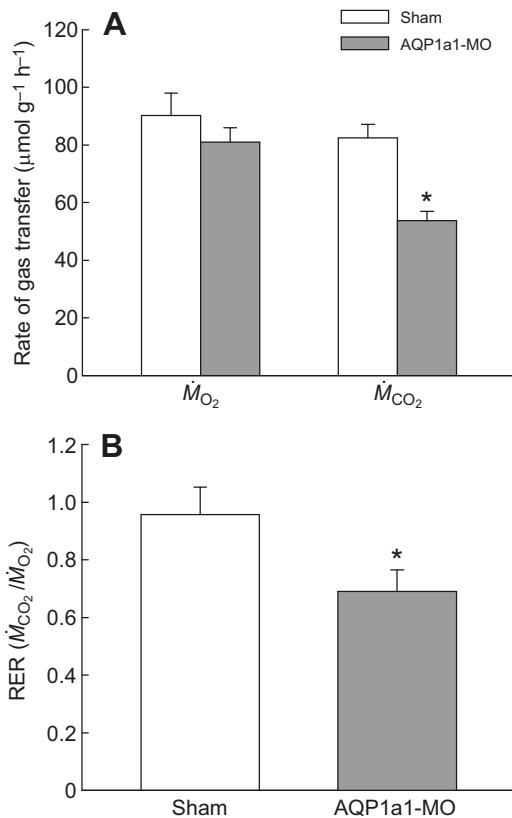


**Fig. 2. Effect of AQP1a1 knockdown on rates of  $\text{O}_2$  uptake and  $\text{CO}_2$  excretion, and the respiratory exchange ratio in 4 dpf zebrafish (*Danio rerio*) larvae (series I).** (A) Rates of  $\text{O}_2$  uptake and  $\text{CO}_2$  excretion, and (B) the RER. Values are means+s.e.m.,  $N=7$ . Significant differences exist between sham and AQP1a1 morphant (AQP1a1-MO) larvae for  $\dot{M}_{\text{CO}_2}$  (\* $P<0.001$ ) and RER (\* $P=0.047$ ) but not  $\dot{M}_{\text{O}_2}$  ( $P=0.331$ ).

### Series II: distinguishing between possible sites of AQP1a1-facilitated gas movement

Immunohistochemistry and confocal microscopy revealed that in addition to the AQP1a1 expressed in HR and NaR ionocytes of the yolk sac epithelium documented by Kwong et al. (2013), AQP1a1 was present in RBCs of 4 dpf larvae (Fig. 4). To assess the contribution of RBC AQP1a1 to  $\text{CO}_2$  and ammonia excretion, haemolytic anaemia was induced by means of PHZ treatment. The effectiveness of PHZ treatment was apparent from the marked loss of globin-specific *o*-dianisidine staining in the heart and trunk vasculature of PHZ-treated relative to control larvae (Fig. 5). If the contribution of RBC AQP1a1 is physiologically relevant, then RBC elimination would be predicted to reduce  $\text{CO}_2$  and/or ammonia excretion. However, no effect of PHZ treatment on  $\dot{M}_{\text{O}_2}$  ( $P=0.506$ ),  $\dot{M}_{\text{CO}_2}$  ( $P=0.658$ ), RER ( $P=0.266$ ) or  $J_{\text{amm}}$  ( $P=0.848$ ) was detected (Fig. 6; two-way ANOVAs). As in series I,  $\dot{M}_{\text{CO}_2}$  ( $P<0.001$ ), RER ( $P<0.001$ ) and  $J_{\text{amm}}$  ( $P<0.001$ ) were significantly lower in AQP1a1-MO relative to sham larvae. In contrast to the lack of effect of AQP1a1 knockdown on  $\dot{M}_{\text{O}_2}$  in series I, a slight but significant ( $P=0.03$ ) reduction in  $\dot{M}_{\text{O}_2}$  was observed in AQP1a1-MO relative to sham larvae (Fig. 6A). The magnitude of the reduction in  $\dot{M}_{\text{CO}_2}$  was, however, about 2.5-fold greater than the decrease in  $\dot{M}_{\text{O}_2}$ , yielding the fall in RER and supporting a specific effect of AQP1a1 knockdown on  $\text{CO}_2$  excretion. No significant interaction between PHZ treatment and AQP1a1 knockdown was detected for any variable ( $P=0.508$  for  $\dot{M}_{\text{O}_2}$ ,  $P=0.255$  for  $\dot{M}_{\text{CO}_2}$ ,  $P=0.366$  for RER and  $P=0.31$  for  $J_{\text{amm}}$ ).

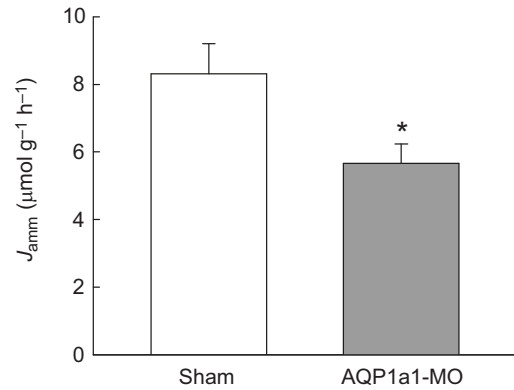


**Fig. 3. Effect of AQP1a1 knockdown on ammonia excretion in 4 dpf zebrafish (*Danio rerio*) larvae (series I).** Values are means+s.e.m.,  $N=12-13$ . Asterisk indicates significant difference between sham and AQP1a1 morphant (AQP1a1-MO) larvae (Student's *t*-test, \* $P=0.018$ ).

### Series III: is there a functional relationship between AQP1a1 and Rhcg1?

The potential for interactions between AQP1a1 and Rhcg1 was examined by measuring, in mirrored experiments, AQP1a1 expression in Rhcg1-MO larvae, and Rhcg1 expression in AQP1a1-MO larvae. Effective knockdown of Rhcg1 was confirmed by measuring  $J_{\text{amm}}$ , which was significantly lower in Rhcg1-MO than sham larvae ( $3.34\pm 0.72$  in Rhcg1-MO versus  $5.80\pm 0.44 \mu\text{mol g}^{-1} \text{h}^{-1}$  in sham larvae,  $N=4$  in each case;  $P=0.027$ , Student's *t*-test). The abundances of AQP1a1 mRNA and protein were not significantly increased in Rhcg1-MO compared with sham larvae (Fig. S1A,B;  $P>0.05$  in both cases, one-sample Student's *t*-tests). Similarly, no significant differences in Rhcg1 protein or mRNA abundance were observed in AQP1a1-MO relative to sham larvae (Fig. S1C,D;  $P>0.05$  in both cases, one-sample Student's *t*-tests).

### Series IV: challenging AQP1a1 with exposure to high external ammonia

Exposure of wild-type larvae to HEA from 1 to 4 dpf had no significant impact on AQP1a1 mRNA or protein abundance (Fig. 7A,B;  $P>0.05$  in both cases, one-sample Student's *t*-tests); a similar lack of effect of HEA exposure on *aqp1a1* mRNA abundance was apparent in sham larvae (Fig. 7A;  $P>0.05$ , one-sample Student's *t*-test). However, in larvae experiencing knockdown of Rhcg1, exposure to HEA resulted in significantly higher AQP1a1 mRNA and protein abundances (Fig. 7A,B;  $P=0.012$  for mRNA, one-sample Student's *t*-test;  $P=0.031$  for protein, one-tailed one-sample Student's *t*-test).

## DISCUSSION

The results of the present study suggest a physiologically significant role for aquaporins beyond their traditional osmoregulatory function. Specifically, the data demonstrate that AQP1a1 is involved in  $\text{CO}_2$  and ammonia excretion in larval zebrafish, adding new roles for this membrane channel to prior work that implicated it in transcellular water uptake *in vivo* in larval zebrafish (Kwong et al., 2013). Because Rh glycoproteins were previously identified as contributing to  $\text{CO}_2$  (Perry et al., 2010) as well as ammonia (Nakada et al., 2007; Shih et al., 2008; Braun et al., 2009a) movements in larval zebrafish, the present study explored the potential for interactions between AQP1a1 and Rhcg1. However, support for the hypothesis that AQP1a1 and Rhcg1 act in concert to

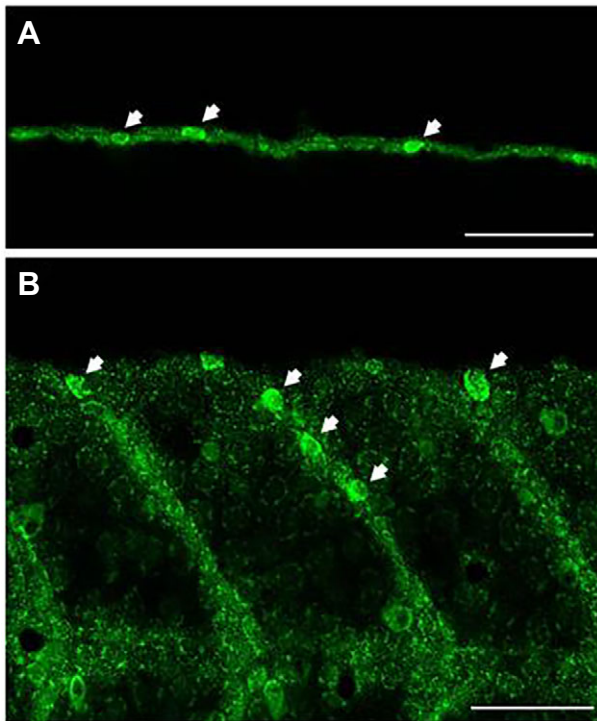


**Fig. 4. Fluorescent immunohistochemistry and confocal microscopy reveals the expression of AQP1a1 in red blood cells (series II).** (A) Dorsal view of the trunk region of a wild-type 4 dpf zebrafish (*Danio rerio*) larva focused on the dorsal longitudinal anastomotic vessel. (B) Lateral view of the trunk showing intersegmental vessels. Arrows indicate AQP1a1 expression in red blood cells. Scale bars: 50  $\mu\text{m}$ .

facilitate  $\text{CO}_2$  and  $\text{NH}_3$  excretion was limited. Beyond providing *in vivo* data supporting a role for AQP1 in gas transfer to the scant number of such studies in the literature, the findings of the present study support current models postulating that gas transfer during early development in teleost fish occurs by diffusion across the body surface and is not reliant on circulating RBCs (see Brauner and Rombough, 2012).

Expression of zebrafish *aqp1a1* in *Xenopus* oocytes established that AQP1a1 was capable of conducting both  $\text{CO}_2$  and ammonia

(Chen et al., 2010). Translational knockdown of AQP1a1 in the present study produced significant and specific reductions in whole-body  $\dot{M}_{\text{CO}_2}$  as well as  $J_{\text{amm}}$ , demonstrating that AQP1a1 serves *in vivo* as a dual  $\text{CO}_2$ -ammonia channel of physiological significance to gas transfer. Like other aquaporins, AQP1 assembles in the plasma membrane as a homotetramer, with each monomer acting as an independent water channel and a larger hydrophobic pore forming at the centre of the tetrameric arrangement (Walz et al., 1997). Water molecules pass through the hydrophilic aquapore of each monomer in single file. Selectivity is conferred by two conserved asparagine-proline-alanine (NPA) motifs located at the centre of the monomer and an aromatic/arginine (ar/R) constriction that forms the narrowest part of the channel (Tajkhorshid et al., 2002; Krenc et al., 2014). As a linear molecule with a diameter similar to that of water,  $\text{CO}_2$  is expected to be capable of passing through the aquapores, although the ar/R constriction poses a significant barrier to  $\text{CO}_2$  movement (Hub and de Groot, 2006; Wang et al., 2007). The hydrophobic central pore appears to provide an energetically more favourable route for  $\text{CO}_2$  movement (Hub and de Groot, 2006; Wang et al., 2007). Ammonia resembles water in size and polarity and should be able to move through the aquapores, but does not permeate through the ar/R constriction as efficiently as water (Krenc et al., 2014). Given that the substrate specificity of zebrafish aquaporins in general is similar to that of their tetrapod counterparts (Tingaud-Sequeira et al., 2010), it is likely that  $\text{CO}_2$  and ammonia traverse zebrafish AQP1a1 through pathways similar to those predicted for AQP1 from other species. However, additional work is needed to test this prediction.

Theoretical considerations argue that aquaporins can make a significant contribution to  $\text{CO}_2$  movement only when the non-gas-channel component of the membrane offers relatively high resistance to  $\text{CO}_2$  diffusion (Wang et al., 2007; Boron et al., 2011; Endeward et al., 2014). Recent work points to cholesterol content as a key regulator of membrane  $\text{CO}_2$  permeability (Itel et al., 2012; Tsiavalariis et al., 2015). In this context, the significant impairment of  $\text{CO}_2$  excretion reported in the present study in zebrafish larvae experiencing AQP1a1 knockdown suggests that membrane cholesterol content warrants investigation. The abundance of gas-permeable membrane channels is the second key regulator of membrane permeability to  $\text{CO}_2$  (Itel et al., 2012). In larval zebrafish, AQP1a1 is expressed in several membranes of

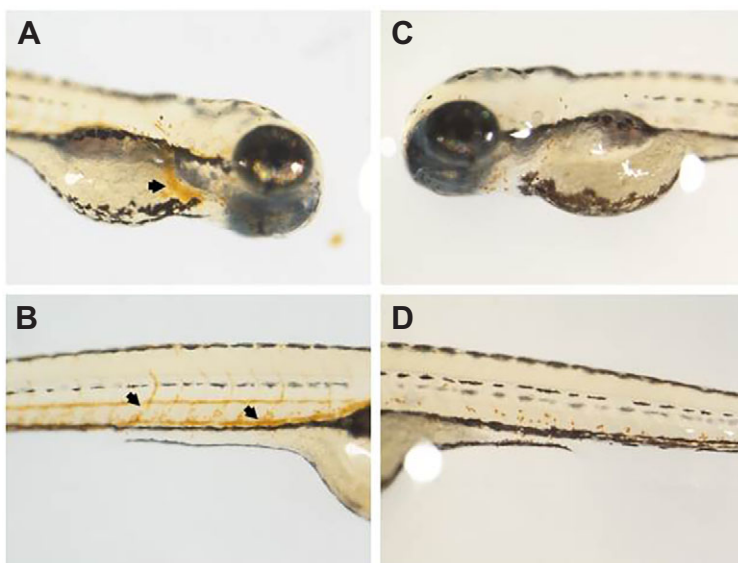


**Fig. 5. Staining with o-dianisidine, a globin-specific dye that functions as a red blood cell marker.** Staining with o-dianisidine in the heart (A, arrow) and trunk vasculature (B, arrows) of control 4 dpf zebrafish (*Danio rerio*) larvae is largely eliminated in animals treated with phenylhydrazine (C,D) to induce haemolytic anaemia (series II).

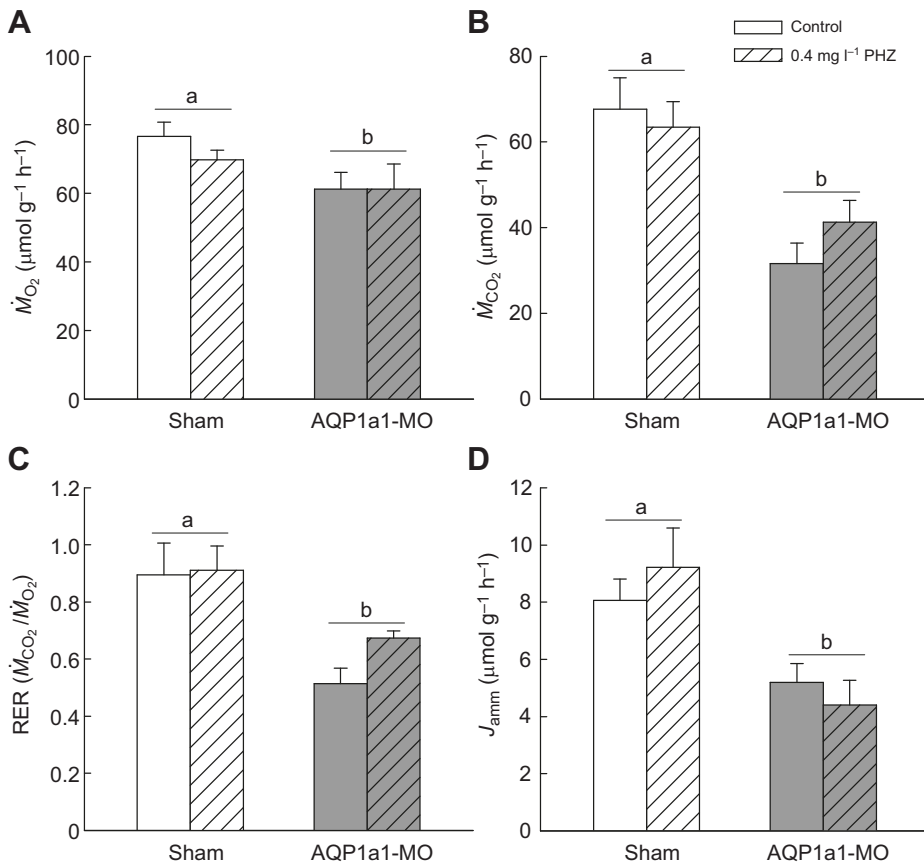


**Fig. 6. Effects of phenylhydrazine treatment on the rate of O<sub>2</sub> uptake, rate of CO<sub>2</sub> excretion, the respiratory exchange ratio and ammonia excretion in 4 dpf sham and morphant larvae (series II).** PHZ treatment effects on (A)  $\dot{M}_{O_2}$ , (B)  $\dot{M}_{CO_2}$ , (C) RER and (D)  $J_{\text{amm}}$  in 4 dpf sham or AQP1a1 morphant (AQP1a1-MO) larvae. Values are means+s.e.m., *N*=5. Groups that share a letter are not significantly different from one another (two-way ANOVA, see text for details).

potential relevance to CO<sub>2</sub> excretion, including endothelial cells of the arterial vasculature (Rehn et al., 2011), RBCs (present study; Chen et al., 2010) and ionocytes of the yolk sac epithelium (Chen

et al., 2010; Kwong et al., 2013). Loss of RBCs, and hence RBC AQP1a1, by treating the developing zebrafish with phenylhydrazine had no significant impact on CO<sub>2</sub> excretion, and AQP1a1

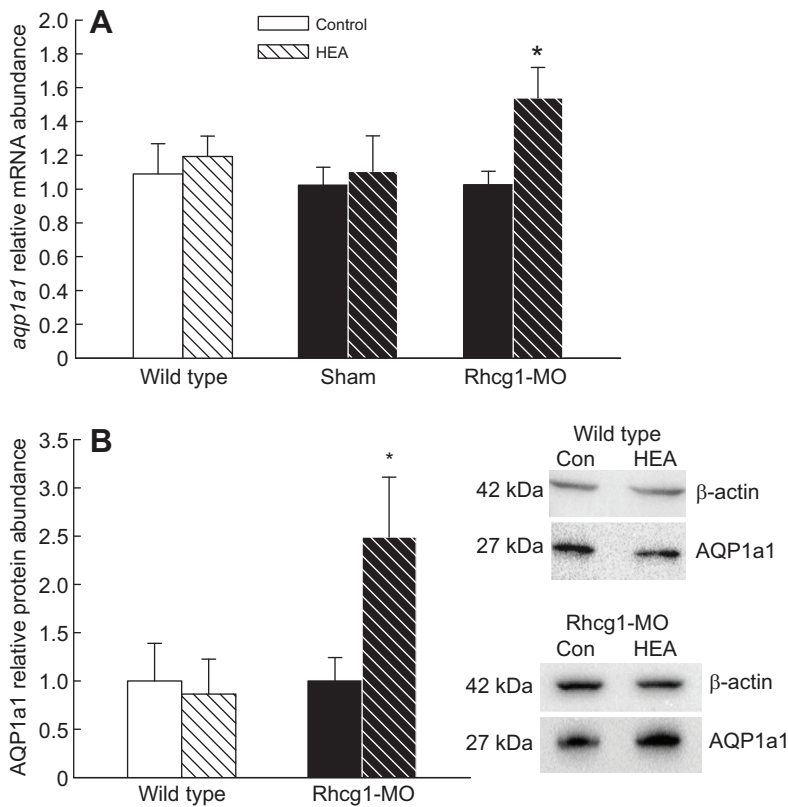


**Fig. 7. Effects of exposure to high external ammonia on relative abundance of AQP1a1 mRNA and protein in 4 dpf larvae (series IV).** HEA exposure effects on relative abundance of AQP1a1 (A) mRNA and (B) protein in wild type, sham or Rhcg1 morphant (Rhcg1-MO) 4 dpf larvae. Values are means+s.e.m., *N*=6–8 with the exception of mRNA abundance in Rhcg1-MO larvae, where *N*=11–12. Values were normalized relative to 18S (for mRNA) or β-actin (for protein), and values for HEA-exposed larvae then were expressed relative to those of the corresponding control group. A significant effect of HEA exposure was observed only in Rhcg1-MO (one-sample Student's *t*-tests, \**P*=0.012 in A and \**P*=0.031 for a one-tailed test in B). The inset in B shows bands from representative western blots illustrating the protein expression of AQP1a1 in lysates of control versus HEA-exposed wild type and Rhcg1-MO larvae relative to corresponding protein expression of β-actin.

knockdown continued to decrease CO<sub>2</sub> excretion in the RBC-deficient larvae, eliminating RBC AQP1a1 as a significant site of CO<sub>2</sub> excretion. A small but significant reduction in metabolic rate (measured as  $\dot{M}_{O_2}$ ) was detected in AQP1a1 morphant larvae in this experimental series, in contrast to the experiments of series I. The reason for this difference between experimental series was not obvious, but a specific effect of AQP1a1 knockdown on CO<sub>2</sub> excretion was still apparent in the significant lowering of the RER.

Although RBCs in conjunction with the gill epithelium play a critical role in CO<sub>2</sub> excretion in adult fish (Perry and Gilmour, 2006), respiratory gas movement is expected to occur cutaneously in embryos and larvae owing to their favourable surface area to volume ratio and thin integument (Brauner and Rombough, 2012). The observation that RBC loss had no impact on either CO<sub>2</sub> excretion or O<sub>2</sub> uptake in the present study supports this model. Previous studies using phenylhydrazine to eliminate RBCs or functional ablation of haemoglobin with carbon monoxide similarly have concluded that RBCs are not needed for O<sub>2</sub> uptake during the early stages of zebrafish development (Pelster and Burggren, 1996; Rombough and Drader, 2009). Fewer studies have focused on CO<sub>2</sub> excretion. However, knockdown of RBC carbonic anhydrase (zCAB), an enzyme that plays a key role in CO<sub>2</sub> excretion via RBCs (Perry and Gilmour, 2006), had no significant impact on CO<sub>2</sub> excretion or RER in zebrafish larvae at 4 dpf (N. Koudrina, S.F.P. and K.M.G., unpublished observations), providing further support for the lack of importance of RBCs to gas transfer during the early stages of zebrafish development. Interestingly, knockdown of zCAB significantly decreased CO<sub>2</sub> excretion at 2 dpf, as did knockdown of the second cytosolic CA isoform in zebrafish, zCAc (Gilmour et al., 2009). The latter isoform is expressed in a wide range of tissues, including ionocytes of the yolk sac epithelium (Lin et al., 2008), but would not be expected to play a role in CO<sub>2</sub> excretion based on current models (Perry and Gilmour, 2006). These discrepant findings suggest that our understanding of CO<sub>2</sub> excretion during the early stages of zebrafish development remains incomplete.

Thus, the AQP1a1 of the yolk sac epithelium is likely to be the significant contributor to CO<sub>2</sub> excretion in 4 dpf zebrafish. In the yolk sac epithelium, AQP1a1 was localized to the basolateral membrane of HR cells and NaR cells (Kwong et al., 2013). The HR cell also expresses apical Rhcg1 (Nakada et al., 2007), which has a well-established role as a selective ammonia transporter in zebrafish larvae (Nakada et al., 2007; Shih et al., 2008, 2013; Braun et al., 2009a) and was recently also implicated in CO<sub>2</sub> excretion (Perry et al., 2010). The findings of the present study suggest that AQP1a1 serves not only as a route for CO<sub>2</sub> excretion, but also as a pathway for ammonia movement. Although *in vitro* work supports the movement of ammonia through AQP1 (Musa-Aziz et al., 2009; Geyer et al., 2013a), the present study appears to be the first to have assessed the contribution of an AQP isoform to elimination of nitrogenous waste *in vivo* in a whole animal. Its location in the basolateral membrane suggests that AQP1a1 may provide a route for the entry of molecular CO<sub>2</sub> and NH<sub>3</sub> gases into ionocytes of the yolk sac epithelium, with exit to the external environment accomplished via apical Rhcg1 and/or diffusion through the lipid bilayer, depending on cell type. For HR cells, an alternative possibility exists: AQP1a1 may contribute to ammonia excretion by facilitating CO<sub>2</sub> entry into the cell. The HR cell appears to have an elevated capacity to excrete ammonia (Shih et al., 2013), likely by virtue of the ‘acid-trapping’ mechanism that can take advantage of H<sup>+</sup> excretion by these cells (Shih et al., 2008; Wright and Wood, 2009; Kumai and Perry, 2011). Ammonia exiting the apical membrane of HR cells via Rhcg1 encounters H<sup>+</sup> extruded by apical V-type H<sup>+</sup>-

ATPase and/or NHE3b, which is responsible for H<sup>+</sup> extrusion coupled to Na<sup>+</sup> uptake (Yan et al., 2007), allowing the formation of NH<sub>4</sub><sup>+</sup>; this effect maintains the outwardly directed NH<sub>3</sub> gradient necessary for excretion (Wright and Wood, 2009). The protons extruded by apical proton pumps and/or NHE3b are the product of CA-catalysed intracellular hydration of CO<sub>2</sub> (Wright and Wood, 2009; Gilmour and Perry, 2009). By facilitating entry of CO<sub>2</sub> into the cell, AQP1a1 could contribute indirectly, but in a significant fashion, to ammonia excretion. The data of the present study do not allow the relative importance of these two mechanisms to be assessed.

Regardless of whether AQP1a1 contributes to ammonia excretion by HR cells directly as an ammonia channel or indirectly as a CO<sub>2</sub> channel, the involvement of Rhcg1 and AQP1a1 in excretion of both CO<sub>2</sub> and ammonia raises the question of whether these two proteins act in concert. Experimental support for this hypothesis was, however, weak. Knockdown of either gas channel did not result in a significant increase in the mRNA or protein expression of the other gas channel under normal conditions, perhaps because knockdown was not complete, so that the stimulus to increase expression was not sufficient. In support of the possibility of coordinated activities of AQP1a1 and Rhcg1, the abundances of AQP1a1 mRNA and protein were significantly elevated in Rhcg1 morphants exposed to HEA, although not in wild-type larvae exposed to HEA. Braun et al. (2009b) demonstrated that HEA significantly reduced ammonia excretion in 4 dpf zebrafish larvae, resulting in accumulation of tissue ammonia levels and compensatory increases in *rhcg1* mRNA expression, presumably to enhance the capacity for ammonia excretion. This apparent reserve capacity for elevating ammonia excretion within the Rh family (Braun et al., 2009b; Shih et al., 2013) may explain why HEA did not affect AQP1a1 expression in wild-type larvae. Knockdown of Rhcg1, by placing constraints on ammonia excretion under conditions of enhanced demand for ammonia excretion, may have provided a sufficient stimulus to increase AQP1a1 mRNA and protein expression.

Freshwater teleosts, by virtue of being hyperosmotic to their environment, face the challenge of constant osmotic influx of water (e.g. Evans et al., 2005). Consequently, the presence of AQP1a1 in ionocytes of the yolk sac epithelium in larval zebrafish is somewhat puzzling – attempts to limit water influx, for example by limiting AQP1a1 expression in the integument, would instead be expected. Indeed, water influx was reduced by 30–58% in zebrafish larvae experiencing AQP1a1 knockdown (present study; Kwong et al., 2013). Kwong et al. (2013) suggested that AQP1a1 plays a role in regulating cell volume in the ionocytes that express it. The significant reductions in CO<sub>2</sub> and ammonia excretion reported in the present study for AQP1a1 morphant larvae provide an additional, compelling reason for AQP1a1 to be present in ionocytes of the yolk sac epithelium. That is, AQP1a1 plays a physiologically relevant role in CO<sub>2</sub> and nitrogenous waste excretion by serving as a gas channel to facilitate the movement of CO<sub>2</sub> and/or ammonia across the integument.

#### Acknowledgements

We are very grateful to Dr Gordon Cramb (University of St Andrews, Scotland) for providing us with the AQP1 antibody and to Prof. Shigehisa Hirose (Tokyo Institute of Technology, Japan) for the Rhcg1 antibody. Thanks are extended to Julia Bradshaw, Yusuke Kumai and Jacob Pollack for technical assistance, to Vishal Saxena and Bill Fletcher for their excellent care of the zebrafish in the aquatic facility, and to Michael Murphy for construction of the total CO<sub>2</sub> analyser.

#### Competing interests

The authors declare no competing or financial interests.

**Author contributions**

S.F.P. and K.M.G. conceived of and designed the experimental approach. K.T. and R.W.M.K. performed the experiments. The original manuscript was derived from the MSc thesis of K.T. by K.M.G. All authors contributed to revising the original manuscript.

**Funding**

The research was supported by Natural Sciences and Engineering Research Council (NSERC) of Canada Discovery and Research Tools and Instruments grants to K.M.G. and S.F.P.

**Supplementary information**

Supplementary information available online at <http://jeb.biologists.org/lookup/suppl/doi:10.1242/jeb.129759/-DC1>

**References**

- Boron, W. F.** (2010). Sharpey-Schafer lecture: gas channels. *Exp. Physiol.* **95**, 1107-1130.
- Boron, W. F., Endeward, V., Gros, G., Musa-Aziz, R. and Pohl, P.** (2011). Intrinsic CO<sub>2</sub> permeability of cell membranes and potential biological relevance of CO<sub>2</sub> channels. *ChemPhysChem* **12**, 1017-1019.
- Boutilier, R. G., Heming, T. A. and Iwama, G. K.** (1984). Appendix: physicochemical parameters for use in fish respiratory physiology. In *Fish Physiology* (ed. W. S. Hoar and D. J. Randall), pp. 403-430. London: Academic Press, Inc.
- Braun, M. H., Steele, S. L., Ekker, M. and Perry, S. F.** (2009a). Nitrogen excretion in developing zebrafish (*Danio rerio*): a role for Rh proteins and urea transporters. *Am. J. Physiol.* **296**, F994-F1005.
- Braun, M. H., Steele, S. L. and Perry, S. F.** (2009b). The responses of zebrafish (*Danio rerio*) to high external ammonia and urea transporter inhibition: nitrogen excretion and expression of rhesus glycoproteins and urea transporter proteins. *J. Exp. Biol.* **212**, 3846-3856.
- Brauner, C. J. and Rombough, P. J.** (2012). Ontogeny and paleophysiology of the gill: new insights from larval and air-breathing fish. *Respir. Physiol. Neurobiol.* **184**, 293-300.
- Chen, L.-M., Zhao, J., Musa-Aziz, R., Pelletier, M. F., Drummond, I. A. and Boron, W. F.** (2010). Cloning and characterization of a zebrafish homologue of human AQP1: a bifunctional water and gas channel. *Am. J. Physiol.* **299**, R1163-R1174.
- de Groot, B. L. and Hub, J. S.** (2011). A decade of debate: significance of CO<sub>2</sub> permeation through membrane channels still controversial. *ChemPhysChem* **12**, 1021-1022.
- Detrich, H. W., Kieran, M. W., Chan, F. Y., Barone, L. M., Yee, K., Rundstadler, J. A., Pratt, S., Ransom, D. and Zon, L. I.** (1995). Intraembryonic hematopoietic cell migration during vertebrate development. *Proc. Natl. Acad. Sci. USA* **92**, 10713-10717.
- Endeward, V., Al-Samir, S., Itel, F. and Gros, G.** (2014). How does carbon dioxide permeate cell membranes? A discussion of concepts, results and methods. *Front. Physiol.* **4**, 382.
- Evans, D. H., Piermarini, P. M. and Choe, K. P.** (2005). The multifunctional fish gill: dominant site of gas exchange, osmoregulation, acid-base regulation, and excretion of nitrogenous waste. *Physiol. Rev.* **85**, 97-177.
- Fang, X., Yang, B., Matthay, M. A. and Verkman, A. S.** (2002). Evidence against aquaporin-1-dependent CO<sub>2</sub> permeability in lung and kidney. *J. Physiol.* **542**, 63-69.
- Geyer, R. R., Musa-Aziz, R., Qin, X. and Boron, W. F.** (2013a). Relative CO<sub>2</sub>/NH<sub>3</sub> selectivities of mammalian aquaporins 0-9. *Am. J. Physiol.* **304**, C985-C994.
- Geyer, R. R., Parker, M. D., Toye, A. M., Boron, W. F. and Musa-Aziz, R.** (2013b). Relative CO<sub>2</sub>/NH<sub>3</sub> permeabilities of human RhAG, RhBG and RhCG. *J. Membr. Biol.* **246**, 915-926.
- Gilmour, K. M. and Perry, S. F.** (2009). Carbonic anhydrase and acid-base regulation in fish. *J. Exp. Biol.* **212**, 1647-1661.
- Gilmour, K. M., Thomas, K., Esbaugh, A. J. and Perry, S. F.** (2009). Carbonic anhydrase expression and CO<sub>2</sub> excretion during early development in zebrafish *Danio rerio*. *J. Exp. Biol.* **212**, 3837-3845.
- Hub, J. S. and de Groot, B. L.** (2006). Does CO<sub>2</sub> permeate through aquaporin-1? *Biophys. J.* **91**, 842-848.
- Itel, F., Al-Samir, S., Öberg, F., Chami, M., Kumar, M., Supuran, C. T., Deen, P. M. T., Meier, W., Hedfalk, K., Gros, G. et al.** (2012). CO<sub>2</sub> permeability of cell membranes is regulated by membrane cholesterol and protein gas channels. *FASEB J.* **26**, 5182-5191.
- Krenc, D., Song, J., Almasalmeh, A., Wu, B. and Beitz, E.** (2014). The arginine-facing amino acid residue of the rat aquaporin 1 constriction determines solute selectivity according to its size and lipophilicity. *Mol. Membr. Biol.* **31**, 228-238.
- Kumai, Y. and Perry, S. F.** (2011). Ammonia excretion via Rhcg1 facilitate Na<sup>+</sup> uptake in larval zebrafish, *Danio rerio*, in acidic water. *Am. J. Physiol.* **301**, R1517-R1528.
- Kwong, R. W. M., Kumai, Y. and Perry, S. F.** (2013). The role of aquaporin and tight junction proteins in the regulation of water movement in larval zebrafish (*Danio rerio*). *PLoS ONE* **8**, e70764.
- Lin, T.-Y., Liao, B.-K., Horng, J.-L., Yah, J.-J., Hsiao, C.-D. and Hwang, P.-P.** (2008). Carbonic anhydrase 2-like a and 15a are involved in acid-base regulation and Na<sup>+</sup> uptake in zebrafish H<sup>+</sup>-ATPase-rich cells. *Am. J. Physiol.* **294**, C1250-C1260.
- Missner, A. and Pohl, P.** (2009). 110 years of the Meyer-Overton rule: predicting membrane permeability of gases and other small compounds. *ChemPhysChem* **10**, 1405-1414.
- Musa-Aziz, R., Chen, L.-M., Pelletier, M. F. and Boron, W. F.** (2009). Relative CO<sub>2</sub>/NH<sub>3</sub> selectivities of AQP1, AQP4, AQP5, AmtB, and RhAG. *Proc. Natl. Acad. Sci. USA* **106**, 5406-5411.
- Nakada, T., Hoshijima, K., Esaki, M., Nagayoshi, S., Kawakami, K. and Hirose, S.** (2007). Localization of ammonia transporter Rhcg1 in mitochondrion-rich cells of yolk sac, gill, and kidney of zebrafish and its ionic strength-dependent expression. *Am. J. Physiol.* **293**, R1743-R1753.
- Pelster, B. and Burggren, W. W.** (1996). Disruption of hemoglobin oxygen transport does not impact oxygen-dependent physiological processes in developing embryos of zebra fish (*Danio rerio*). *Circ. Res.* **79**, 358-362.
- Perry, S. F. and Gilmour, K. M.** (2006). Acid-base balance and CO<sub>2</sub> excretion in fish: unanswered questions and emerging models. *Respir. Physiol. Neurobiol.* **154**, 199-215.
- Perry, S. F., Braun, M. H., Noland, M., Dawdy, J. and Walsh, P. J.** (2010). Do zebrafish Rh proteins act as dual ammonia-CO<sub>2</sub> channels? *J. Exp. Zool. A Ecol. Genet. Physiol.* **313A**, 618-621.
- Pfaffl, M. W.** (2001). A new mathematical model for relative quantification in real-time RT-PCR. *Nucleic Acids Res.* **29**, e45.
- Rehn, K., Wong, K. S., Balciunas, D. and Sumanas, S.** (2011). Zebrafish enhancer trap line recapitulates embryonic aquaporin 1a expression pattern in vascular endothelial cells. *Int. J. Dev. Biol.* **55**, 613-618.
- Rombough, P.** (2002). Gills are needed for ionoregulation before they are needed for O<sub>2</sub> uptake in developing zebrafish, *Danio rerio*. *J. Exp. Biol.* **205**, 1787-1794.
- Rombough, P. and Drader, H.** (2009). Hemoglobin enhances oxygen uptake in larval zebrafish (*Danio rerio*) but only under conditions of extreme hypoxia. *J. Exp. Biol.* **212**, 778-784.
- Shih, T.-H., Horng, J.-L., Hwang, P.-P. and Lin, L.-Y.** (2008). Ammonia excretion by the skin of zebrafish (*Danio rerio*) larvae. *Am. J. Physiol.* **295**, C1625-C1632.
- Shih, T.-H., Horng, J.-L., Lai, Y.-T. and Lin, L.-Y.** (2013). Rhcg1 and Rhbg mediate ammonia excretion by ionocytes and keratinocytes in the skin of zebrafish larvae: H<sup>+</sup>-ATPase-linked active ammonia excretion by ionocytes. *Am. J. Physiol.* **304**, R1130-R1138.
- Tajkhorshid, E., Nollert, P., Jensen, M. Ø., Miercke, L. J. W., O'Connell, J., Stroud, R. M. and Schulten, K.** (2002). Control of the selectivity of the aquaporin water channel family by global orientation tuning. *Science* **296**, 525-530.
- Tingaud-Sequeira, A., Calusinska, M., Finn, R. N., Chauvigné, F., Lozano, J. and Cerdà, J.** (2010). The zebrafish genome encodes the largest vertebrate repertoire of functional aquaporins with dual paralogy and substrate specificities similar to mammals. *BMC Evol. Biol.* **10**, 38.
- Tsiavalariis, G., Itel, F., Hedfalk, K., Al-Samir, S., Meier, W., Gros, G. and Endeward, V.** (2015). Low CO<sub>2</sub> permeability of cholesterol-containing liposomes detected by stopped-flow fluorescence spectroscopy. *FASEB J.* **29**, 1780-1793.
- Uehlein, N., Lovisolo, C., Siefert, F. and Kaldenhoff, R.** (2003). The tobacco aquaporin NTAQP1 is a membrane CO<sub>2</sub> pore with physiological functions. *Nature* **425**, 734-737.
- Verdouw, H., van Eched, C. J. A. and Dekkers, E. M. J.** (1978). Ammonia determination based on indophenol formation with sodium salicylate. *Water Res.* **12**, 399-402.
- Walz, T., Hirai, T., Murata, K., Heymann, J. B., Mitsuoka, K., Fujiyoshi, Y., Smith, B. L., Agre, P. and Engel, A.** (1997). The three-dimensional structure of aquaporin-1. *Nature* **387**, 624-627.
- Wang, Y., Cohen, J., Boron, W. F., Schulten, K. and Tajkhorshid, E.** (2007). Exploring gas permeability of cellular membranes and membrane channels with molecular dynamics. *J. Struct. Biol.* **157**, 534-544.
- Westerfield, M.** (2000). *The Zebrafish Book. A Guide for the Laboratory use of Zebrafish (Danio rerio)*, 4th edn. Eugene, Oregon: University of Oregon Press.
- Wright, P. A. and Wood, C. M.** (2009). A new paradigm for ammonia excretion in aquatic animals: role of Rhesus (Rh) glycoproteins. *J. Exp. Biol.* **212**, 2303-2312.
- Xu, L., Zhou, Y., Courtney, N. A., Radford, T. S. and Boron, W. F.** (2010). Effect of AQP1 knock out on mouse exercise tolerance. *FASEB J.* **24** Meeting Abstract Suppl., 609.4.

- Yan, J.-J., Chou, M.-Y., Kaneko, T. and Hwang, P.-P.** (2007). Gene expression of  $\text{Na}^+/\text{H}^+$  exchanger in zebrafish  $\text{H}^+$ -ATPase-rich cells during acclimation to low- $\text{Na}^+$  and acidic environments. *Am. J. Physiol. Cell Physiol.* **293**, C1814-C1823.
- Yang, H., Hewett-Emmett, D. and Tashian, R. E.** (2000). Absence or reduction of carbonic anhydrase II in the red cells of the beluga whale and llama: implications for adaptation to hypoxia. *Biochem. Genet.* **38**, 241-252.
- Zapater, C., Chauvigné, F., Norberg, B., Finn, R. N. and Cerdà, J.** (2011). Dual neofunctionalization of a rapidly evolving aquaporin-1 paralog resulted in constrained and relaxed traits controlling channel function during meiosis resumption in teleosts. *Mol. Biol. Evol.* **28**, 3151-3169.
- Zhou, Y., Bouyer, P. and Boron, W. F.** (2006). Evidence that AQP1 is a functional  $\text{CO}_2$  channel in proximal tubules. *FASEB J.* **20** Meeting Abstract Suppl., A1225.